Active feedback stabilization of the flute instability in a mirror machine using field-aligned coils

A. Lifshitz[1]**, I. Be'ery**[1]**, A. Fisher**[1]**, A. Ron**[1] **and A. Fruchtman**[2]

[1] Physics Department, Technion, Haifa 32000, Israel
[2] Faculty of Sciences, HIT-Holon Institute of Technology, Holon 58102, Israel

E-mail: assaf.lif@gmail.com

Abstract

A plasma confined in linear mirror machines is unstable even at low β, mainly because of the flute instability. One possible way to stabilize the plasma is to use active feedback to correct the plasma shape in real time. The theoretically investigated apparatus consists of feedback coils aligned with the magnetic field, immersed in a cold plasma around the hot core. When the current through the feedback coils changes, the plasma moves to conserve the magnetic flux via compressional Alfvén waves. An analytical model is used to find a robust feedback algorithm with zero residual currents. It is shown that due to the plasma's rotation, maximal stability is obtained with a large phase angle between the perturbations' modes and the feedback integral-like term. Finally, a two-dimensional MHD simulation implementing the above algorithm in fact shows stabilization of the plasma with zero residual currents.

(Some figures may appear in colour only in the online journal)

1. Introduction

The flute instability is a large-scale mode through which the plasma escapes an axial mirror machine. The physical mechanism is governed by a positive feedback: each field line in the trap has an average curvature pointing outwards, creating a curvature-driven current. This current creates charge accumulation when the pressure radial symmetry is broken, which creates electrostatic fields, causing $\vec{E} \times \vec{B}$ flow in the radial direction, which tends to increase the pressure asymmetry. In the linear regime, the rate of growth of the asymmetry in the electric field (and pressure distribution) is proportional to the asymmetry of the pressure distribution (and electric field).

The possibility of using active feedback in order to stop the instabilities has been investigated in several works. Starting half a century ago, active feedback stabilization has been suggested as a method to control the growth of flute instability [1–4]. Some of these works considered electrostatic actuators [1, 2], while others looked at magnetic ones [3, 4]. However, all these works used an analytical approach, assuming infinitesimal perturbation amplitudes, de-coupling of the various modes, and other simplifying assumptions. Few experimental efforts [5, 6] demonstrated the possibility of active feedback control in mirror machines, but employed only electrostatic control, on an extremely low-density plasma. While progress in feedback stabilization of

mirror traps has been very slow, active feedback has become a major tool for tokamaks and other toroidal traps. In these machines active feedback is usually applied to relatively slow processes such as vertical stabilization and the resistive wall instability [7, 8].

In this paper, we use an analytical model and a two-dimensional MHD simulation to explore the possibility of driving feedback currents through coils immersed inside a cold plasma, around the hot core, in order to achieve stabilization. These feedback currents result in additional electric fields, associated with excited compressional Alfvén waves, $\vec{E} = -\vec{\nabla}\phi + \vec{E}_{\text{feedback}}$. The feedback currents are chosen so as to create $\vec{E}_{\text{feedback}}$ that restore symmetry.

This work is organized as follows: first, the investigated system and the main assumptions are described. Next, the plasma's response to currents in the feedback coils is calculated. Then, an analytical analysis is employed to choose a feedback algorithm. Finally, the suggested algorithm is tested using a two-dimensional simulation. In conclusion, results and several aspects of applicability are discussed.

2. The investigated system

This work assumes that a plasma is trapped in a mirror machine similar to the GDT (described in [9, 11]), with the addition of feedback coils, as shown in figure 1. Most of the following trap and plasma parameters were chosen to match those of
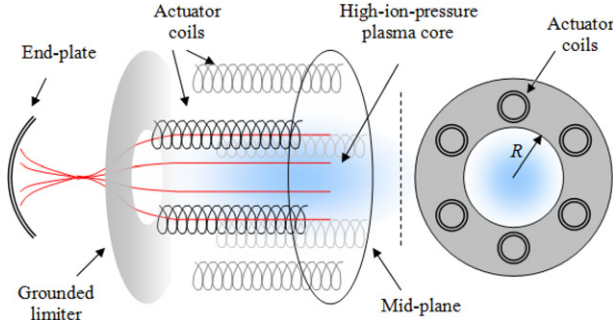
Figure 1. Schematic view of the investigated apparatus. The feedback coils are located around the hot core. Left: perspective view; right: view along the main axis.

GDT. While [9] describes stabilization of GDT with sheared plasma rotation (via biasing of the limiter), this work explores the option of using active feedback.

The trap. The trap length (mirror-to-mirror) is $L = 7\,\mathrm{m}$. The magnetic field is uniform and has a value of $B_0 = 0.3\,\mathrm{T}$. The field lines are straight, except for a relatively small region near the throats, where the field is amplified by the mirror ratio $R_{\mathrm{m}} \approx 20$. A grounded limiter is placed at a radius $R = 10\,\mathrm{cm}$. Any plasma reaching the limiter radius is cooled very fast. At the end of the field lines close to the main axis, there are 'end-plates'. Current from them flows into (or out of) the plasma depending on the potential difference.

The plasma. The micro-instabilities, common in mirror machines, are resolved in the GDT concept by using a plasma with mean free path smaller than the trap's length. Due to the high collisionality, the density and temperature are nearly uniform in the middle section. A plasma of density $n = 3 \times 10^{13}\,\mathrm{cm}^{-3}$ fills the trap, even outside the limiter radius (though it has a much lower ion temperature there). The ion temperature in the hot core is $T_{\mathrm{i}} \approx 1\,\mathrm{keV}$, but the electron temperature is far lower, about $T_{\mathrm{e}} \approx 100\,\mathrm{eV}$. The electron temperature in the core is assumed to be higher by about $20\,\mathrm{eV}$ due to coupling to the hotter ions. This gradient causes a rotation of the plasma due to the radial electric field. While high β values of up to 50% have been reached in GDT in some operations and some regions of the trap, we analyse the much simpler low-β system.

The feedback apparatus. The (theoretically) investigated feedback apparatus consists of $N = 6$ long, thin coils (relative to R), running along the magnetic field lines. The coils are evenly distributed at a distance $r_{\mathrm{coil}} = 13\,\mathrm{cm}$ from the axis of symmetry and at angles $\theta_i = (i/N) \cdot 2\pi$ ($i = 1 \ldots N$). The coils are of radius $R_{\mathrm{coil}} = 1\,\mathrm{cm}$ and have a turn density of $\nu = 100\,\mathrm{turns\,m}^{-1}$. The coils are immersed inside the cold plasma, outside of the limiter radius. The feedback current through the coils changes in response to the plasma shape in a way to achieve stabilization.

3. Plasma's response to the feedback coils

3.1. System infinite in the z-direction

We start by analysing the plasma's response to a single coil, and then to several coils. In order to calculate the plasma's
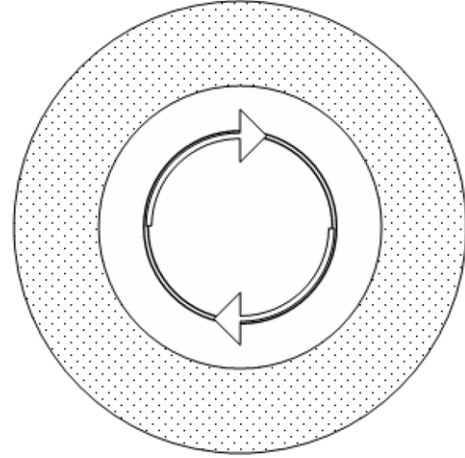
Figure 2. Current (indicated by arrows) running through an infinite coil surrounded by the plasma tube (indicated by the dotted area).

response to current in a single feedback coil, we assume it is of infinite length, and surrounded by a hollow tube of plasma, also of infinite length, as shown in figure 2.

The radius of the coil is R_{coil}, the inner and outer radii of the plasma hollow cylinder are r_{in} and r_{out}, so that $R_{\mathrm{coil}} < r_{\mathrm{in}} < r_{\mathrm{out}}$. The plasma and the coil are immersed in a uniform magnetic field, B_0, which is parallel to the axis of the coil. We also assume the plasma is highly conductive, has uniform density, ρ_0, and with an arbitrary pressure distribution but a low β (plasma pressure/magnetic pressure).

Changes in the current in the coil, $I(t)$, result in currents in the internal plasma surface that act to conserve the magnetic flux. These currents cause plasma displacement via the Lorentz force. Thus, current changes in the coil act as a piston on the internal plasma surface. The velocity gained by the plasma at its internal edge is $\vec{V}(r_{\mathrm{in}}, t) = -(\mu_0 R_{\mathrm{coil}}^2 \nu / 2 B_0 r_{\mathrm{in}})(\mathrm{d}I(t)/\mathrm{d}t)\hat{r}$; the motion compensates for the flux changes from the coil. The magnetic field energy released from the coil is first converted into magnetic field energy (and to a smaller extent into plasma kinetic energy) that propagates inside the plasma as a compressional Alfvén wave with velocity, $v_{\mathrm{A}} = B_0/\sqrt{\mu_0 \rho_0}$. For current changes with a much slower time than the transit time of the wave in the plasma, $t_{\mathrm{d}} = (r_{\mathrm{out}} - r_{\mathrm{in}})/v_{\mathrm{A}}$, the compression is small, and the plasma velocity is approximately $\vec{V}(r, t) = -(\mu_0 R_{\mathrm{coil}}^2 \nu / 2 B_0 r)(\mathrm{d}I(t)/\mathrm{d}t)\hat{r}$. Integrating the velocity, the displacement of each plasma element from its initial location is $\vec{\xi}(r, t) = -(\mu_0 R_{\mathrm{coil}}^2 \nu / 2 B_0 r)I(t)\hat{r}$, and is independent of the plasma mass. For slow current changes, the electric field inside the plasma is

$$\vec{E}(r, t) = -\vec{V} \times \vec{B} = -\frac{\mu_0 R_{\mathrm{coil}}^2 \nu}{2r} \frac{\mathrm{d}I(t)}{\mathrm{d}t}\hat{\theta}, \qquad (1)$$

which, in that limit, is just the induced electric field that would have been generated had there been no plasma. We assume that this result holds for the more general (two-dimensional) case.

The requirements for the above derivation to be valid are that the plasma conductivity is high enough so that the flux is indeed conserved, meaning the magnetic field diffusion is
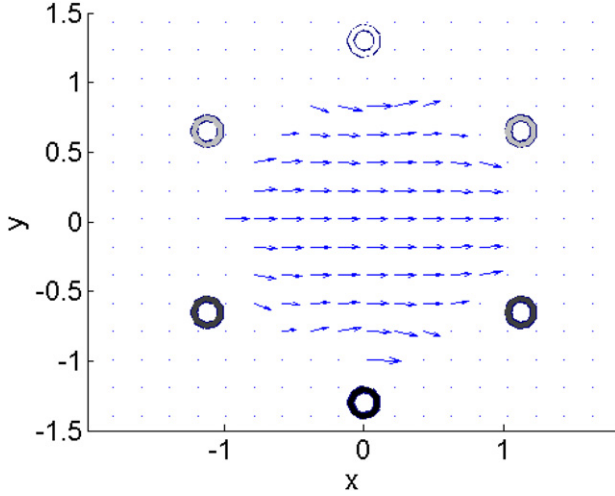
Figure 3. Quiver plot of $\vec{E}_{1,y}$, induced by the ($m = 1$, y) I-dot mode. Distance is normalized by the limiter radius. Grey level of the coils indicates the rate of change of current from the maximal rate (white) to the minimal (and negative) rate (black).

slow. The magnetic field diffusion coefficient, using Spitzer's formula for the plasma conductivity, is $D_{\mathrm{Sp.}} = 1/\mu_0 \sigma_{\mathrm{Sp.}} \approx (T_e \, \mathrm{eV}^{-1})^{-3/2} 60 \, \mathrm{cm}^2 \, \mu \mathrm{s}^{-1}$. For electron temperatures of even $20 \, \mathrm{eV}$, it is $D_{\mathrm{Sp.}} \approx 0.7 \, \mathrm{cm}^2 \, \mu \mathrm{s}^{-1}$, which is low enough for most practical situations.

It is now time to define the feedback modes, or the 'I-dot' modes, prescribing the current's rate of change for each coil:

$$\dot{I}^i_{m,x} = A_{m,x} \cos(m\theta_i), \qquad \dot{I}^i_{m,y} = A_{m,y} \sin(m\theta_i). \quad (2)$$

Here i is the index of the coil and m is the mode number.

In a finite multi-coil system, the electric field of the single coil is distorted by the presence of the other coils and the plasma edge. Given the coils' small radius relative to the distance from each other, and assuming the plasma's external edge is far from the coils' centres, one can assume that the electric fields induced in the plasma by each coil is almost the same as the field of a stand-alone coil, and the fields of all the coils add linearly. Thus, every current mode has an associated electric field $\vec{E}_{m,\xi}$ (with $\xi = x$ or $\xi = y$). A quiver plot of $\vec{E}_{1,y}$ is given as an example in figure 3.

The $A_{m,\xi}$ coefficients are defined to make $\langle \vec{E}_{m,\xi}, \vec{E}_{m',\xi'} \rangle \equiv (1/\pi\phi^2) \int_{r<R} \vec{E}_{m,\xi} \cdot \vec{E}_{m',\xi'} \, dS = \delta_{m,m'} \delta_{\xi,\xi'}$, with ϕ being the floating potential. Thus, the set of functions $\{\vec{E}_{m,\xi}\}$, although not a basis, is orthonormal. The normality is due to the equal angular separation between the coils.

Basically, the feedback-induced field can be used to reverse the electrostatic field in the plasma rising from the flute instability, thus achieving stabilization. We now turn to finding a robust feedback algorithm, making use of the ability to influence the electric field inside the plasma.

3.2. System finite in the z-direction

Any practical system is of course finite in the z-direction. There is thus the question of the effect of the finite size. One such complication is the presence of limiters and end-plates. Since the electric field of the flute is purely electrostatic, the plasma can move across the magnetic field lines without altering the magnetic field at the limiters and end-plates. The electric field of the feedback solenoids, on the other hand, is an inductive one, and therefore might impose a problem at the intersection of the plasma, solenoids and conducting surfaces. This problem can be issued in real experiments in several ways.

- The coils, taken to be infinite in the z-direction in the simulation, can actually end near the mirrors, while the end-plates and limiters are put further out of the mirror (figure 1). If the distance from the end of the coils to the conducting surfaces is larger than the diameter of the coils, the induced field near the end-plates and limiters will be small, while the effect on the plasma will be almost the same.
- The limiters and end-plates can be split in such a way as to prevent induction currents due to the feedback coils. For example, the limiters could be cut by lines running from the centre of the trap to the centre of each feedback coil.
- The limiters might have resistance in the r–θ plane high enough to allow magnetic diffusion on a time scale relevant for the feedback action. At the same time, the resistance has to be low enough to prevent charge accumulation on them.
- If the plasma is long and thin, and if the translations due to the feedback are small, the limiters' effect on the magnetic field lines will be localized and will have small influence on the feedback and flute dynamics.

4. Analytical model of the feedback

As will be shown later, it is necessary to take into account the system's rotation in the design of the feedback. In the absence of external feedback, rotation has a stabilizing effect [9]. In fact, stabilization by strong $\vec{E} \times \vec{B}$-induced rotation has been demonstrated to be very effective [9]. In active feedback stabilization, on the other hand, the rotation can have a destabilizing effect even without a delay between the perturbation and feedback response. Theory and experiments [10, 11] suggest that the growing interchange modes will generally rotate about the trap's axis, and the rotation velocity might be comparable to the growth velocity. The rotation is caused by a drop in the floating potential along the radius, due to gradients in the electron temperature. The rotation frequency can be estimated by

$$\omega_{\mathrm{rot}} \approx \frac{R}{v_{E \times B}} \approx \frac{R}{\phi/RB} = \frac{BR^2}{\phi}.$$

Let us analyse the stabilization of an arbitrary m-mode. For the two spatial components of the mode, we denote the pressure distribution asymmetry of the plasma with the scalars: $\tilde{P}_x = \iint P \cos(m\theta) r \, dr \, d\theta$, $\tilde{P}_y = \iint P \sin(m\theta) r \, dr \, d\theta$. The electric field asymmetry is denoted with the equivalent scalars $\tilde{E}_\xi$. The two fundamental equations describing the instability at the linear phase are $(d/dt) \tilde{P}_\xi = \alpha \tilde{E}_\xi$ and $(d/dt) \tilde{E}_\xi = \beta \tilde{P}_\xi$. These coupled equations are of the exact form as an inverted pendulum, and are unstable with a characteristic frequency of $\omega_0 = (\alpha\beta)^{1/2}$. In this work, we explore the possibility of adding feedback electric fields—$\tilde{E}_{\mathrm{f},x}$ and $\tilde{E}_{\mathrm{f},y}$—on top of the existing one. Thus, the pressure asymmetry changes according to $(d/dt) \tilde{P}_\xi = \alpha (\tilde{E}_\xi + \tilde{E}_{\mathrm{f},\xi})$. Bearing in mind that

the feedback electric field is proportional to the rate of change of the feedback current (see equation (1)), we can substitute $\tilde{E}_{\mathrm{f},\xi}$ for $\mathrm{d}\tilde{I}_\xi/\mathrm{d}t$. Finally, taking into account the system's rotation, the set of coupled equations is

$$\frac{\mathrm{d}}{\mathrm{d}t}\begin{pmatrix}\tilde{P}_x\\\tilde{P}_y\\\tilde{E}_x\\\tilde{E}_y\\\tilde{I}_x\\\tilde{I}_y\end{pmatrix}=\begin{pmatrix}\omega_{\mathrm{rot.}}\tilde{P}_y+\alpha\tilde{E}_x+\alpha E_{\mathrm{f},x}\\-\omega_{\mathrm{rot.}}\tilde{P}_x+\alpha\tilde{E}_y+\alpha E_{\mathrm{f},y}\\\omega_{\mathrm{rot.}}\tilde{E}_y+\beta\tilde{P}_x\\-\omega_{\mathrm{rot.}}\tilde{E}_x+\beta\tilde{P}_y\\E_{\mathrm{f},x}\\E_{\mathrm{f},y}\end{pmatrix}. \qquad (3)$$

The system can be made stable by, for instance, setting $\tilde{E}_{\mathrm{f},\xi}=G\tilde{E}_\xi$, with $G<-1$. This is equivalent to the 'P' term of a proportional–integral–derivative (PID) controller. In this case, the system will just oscillate around its equilibrium. An improvement on this method is to add a term proportional to $\tilde{P}_\xi$: $E_{\mathrm{f},\xi}=G\tilde{E}_\xi+G\tau_{\mathrm{ext.}}\beta\tilde{P}_\xi$. The new term is equivalent to the 'D' term in the PID controller, and acts to temporally extrapolate $\tilde{E}_\xi$. For positive $\tau_{\mathrm{ext.}}$, any perturbation will decay. However, in general, the system may stabilize with $\tilde{I}_\xi\neq 0$. This is undesirable in any practical application. For this reason, it is preferable to add a term proportional to the current. For reasons to be made clear later we make use of both currents:

$$\begin{pmatrix}\tilde{E}_{\mathrm{f},x}\\\tilde{E}_{\mathrm{f},y}\end{pmatrix}=G\begin{pmatrix}\tilde{E}_x\\\tilde{E}_y\end{pmatrix}+G\tau_{\mathrm{ext.}}\beta\begin{pmatrix}\tilde{P}_x\\\tilde{P}_y\end{pmatrix}$$
$$+\,\delta\begin{pmatrix}\cos\psi & \sin\psi\\-\sin\psi & \cos\psi\end{pmatrix}\begin{pmatrix}\tilde{I}_x\\\tilde{I}_y\end{pmatrix}. \qquad (4)$$

Even for zero phase angle $\psi=0$, this is not equivalent to the 'I' term of the PID controller, since I is an integral of the feedback electric field and not the plasma's field.

Since all the feedback terms are linear, equation (3) can be written in a matrix form:

$$\frac{\mathrm{d}}{\mathrm{d}t}\begin{pmatrix}\tilde{P}_x\\\tilde{P}_y\\\tilde{E}_x\\\tilde{E}_y\\\tilde{I}_x\\\tilde{I}_y\end{pmatrix}=\begin{pmatrix}\alpha\beta G\tau_{\mathrm{ext.}} & \omega_{\mathrm{rot.}} & \alpha(G+1) & 0 & \alpha\delta\cos\psi & \alpha\delta\sin\psi\\-\omega_{\mathrm{rot.}} & \alpha\beta G\tau_{\mathrm{ext.}} & 0 & \alpha(G+1) & -\alpha\delta\sin\psi & \alpha\delta\cos\psi\\\beta & 0 & 0 & \omega_{\mathrm{rot.}} & 0 & 0\\0 & \beta & -\omega_{\mathrm{rot.}} & 0 & 0 & 0\\\beta G\tau_{\mathrm{ext.}} & 0 & G & 0 & \alpha\delta\cos\psi & \alpha\delta\sin\psi\\0 & \beta G\tau_{\mathrm{ext.}} & 0 & G & -\alpha\delta\sin\psi & \alpha\delta\cos\psi\end{pmatrix}$$
$$\times\begin{pmatrix}\tilde{P}_x\\\tilde{P}_y\\\tilde{E}_x\\\tilde{E}_y\\\tilde{I}_x\\\tilde{I}_y\end{pmatrix}. \qquad (5)$$

Linear analysis of equation (5) is carried out by assuming $\mathrm{e}^{\mathrm{i}\omega t}$ dependence and solving the eigenvalue problem. In general, there are six different complex values for ω, and it only takes one with a negative imaginary part for the perturbations to grow exponentially. We can define a (possibly negative) decay rate by: $\tau_{\mathrm{decay}}^{-1}\equiv\min\{\mathrm{im}(\omega)\}$. Thus, 'good' feedback parameters are ones that make $\tau_{\mathrm{decay}}^{-1}$ positive, and preferably large.

A 'stability map' is plotted in figure 4, showing the value of $\tau_{\mathrm{decay}}^{-1}$ for different values of δ and ψ. It is evident that for $\psi=0°$ stabilization, although possible, is very difficult to achieve. Around $\psi=\pm90°$, it is relatively easy to achieve stabilization, as can be seen by the wide range of values for δ which still give stabilization. This is desirable, and means that there is no sensitivity to the different physical parameters ($\omega_{\mathrm{rot.}}$ for instance).
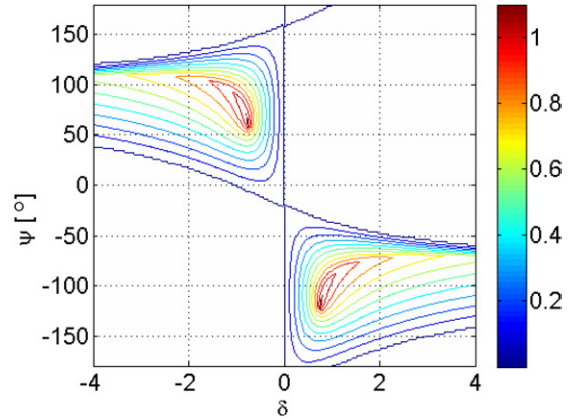
Figure 4. Contour plot of the decay rate, $\tau_{\mathrm{decay}}^{-1}$. Higher values correspond to faster stabilization, and negative values correspond to instability. Negative values are not drawn. The parameters used are $\alpha=\beta=1$, $\omega_{\mathrm{rot.}}=3$, $G=-6$, $\tau_{\mathrm{ext}}=0.8$.

5. Two-dimensional simulation of confinement

5.1. Model equations

The MHD equations derived in [9] were used to simulate confinement. The equations are brought into the dimensionless form, after normalizing with B_0, R, ϕ, p_0, the magnetic field, limiter radius, applied limiter potential and maximal ion pressure, respectively. In this work, there is no applied limiter potential, but rather stabilization is achieved with an active feedback mechanism. Thus, $\phi\approx 50\,\mathrm{V}$ denotes the difference in electron floating potential in the core. The derived variables are normalized by a combination of these parameters. Thus, t is normalized by $\tau=BR^2/\phi$, E is normalized by ϕ/R, I is normalized by $B_0/\mu_0\nu$, etc. In this work, the derivation was repeated, but assuming $\vec{E}=-\vec{\nabla}\varphi+\vec{E}_{\mathrm{feedback}}$ instead of $\vec{E}=-\vec{\nabla}\varphi$, with $\vec{E}_{\mathrm{feedback}}$ being the feedback electric field.

The pressure convection equation remains

$$\frac{\partial p}{\partial t}+\vec{V}_{\vec{E}\times\vec{B}}\cdot\vec{\nabla}p=\nu_\perp\vec{\nabla}^2 p-\nu_\parallel p+Q_p; \qquad (6)$$

only now does the electric field driving the $\vec{V}_{\vec{E}\times\vec{B}}$ term include the induced feedback field.

The equation for the electric potential evolution is again derived by integrating $\vec{\nabla}\cdot\vec{J}=0$ along the field lines. To simplify the resulting equation, we make two observations. The first is that $\vec{\nabla}\cdot\vec{E}_{\mathrm{feedback}}=0$, since the electric field results from currents and not charges (this, of course, can also be verified by using equation (1)). The second is that $\vec{\nabla}\cdot(\vec{E}_{\mathrm{feedback}}\times\vec{B})=\vec{B}\cdot(\vec{\nabla}\times\vec{E}_{\mathrm{feedback}})-\vec{E}_{\mathrm{feedback}}\cdot(\vec{\nabla}\times\vec{B})=0$. This is because outside the coils, in the plasma region, $\vec{\nabla}\times\vec{E}_{\mathrm{feedback}}=0$ (again, as can be verified by equation (1)), and $\vec{\nabla}\times\vec{B}=0$, which is a good approximation for a low-β plasma and time scales slower than the speed of light. Finally, the resulting equation is

$$\partial_t\vec{\nabla}^2\varphi=\vec{\nabla}\cdot((\vec{V}_{\vec{E}\times\vec{B}}\cdot\vec{\nabla})(\vec{E}_{\mathrm{feedback}}-\vec{\nabla}\varphi))+H\cdot(\varphi-\varphi_{\mathrm{w}})$$
$$-\kappa\cdot r\cdot\hat{\theta}\cdot\vec{\nabla}p+\nu_\perp\vec{\nabla}_\perp^2(\vec{\nabla}_\perp^2\varphi)+U\vec{\nabla}\cdot((\vec{\nabla}p\cdot\vec{\nabla})\vec{V}_{\vec{E}\times\vec{B}}),$$
$$\qquad (7)$$

where $H=J_{\mathrm{i}0}\tau^2 B_0^2 e\phi/B_{\mathrm{w}}L\rho T_{\mathrm{e}}$ ($J_{\mathrm{i}0}$ being the ion saturation current and B_{w} the magnetic field at the wall) is the end-plate coupling constant, $\kappa=2p_0\tau^2(\langle g(z)\alpha(z)B^{-1}\rangle/\langle\rho B^{-2}\rangle)$

(with $g(z)$ part of the pressure decomposition $p(r, z) = g(z)p(r)$, and $\alpha(z)$ part of the magnetic field decomposition $1/B(r, z) \approx (1/B(0, z)) + \alpha(z)r^2)$ is the normalized curvature, $\nu_\perp = \eta_i B_0/nm\phi$ (with η_i the ion collisional viscosity) is the perpendicular diffusion coefficient, and $U = p_0/en\phi$ is the finite Larmor radius (FLR) coefficient.

There is a difference in coupling coefficients with respect to [9], due to a much lower value of ϕ (50 V in this work, as opposed to $\sim$200 V). Due to this change, the coupling coefficients are $H = 60$, $\kappa = 25$ and $U = -25$. Variations of these coefficients do not significantly change the results presented in the following sections, as long as the simulated plasma is stable to high mode number instabilities.

Simulations of plasma evolution with and without feedback were carried out by integrating equations (6)–(8). This was performed using MATLAB's 'ode45' routine, with a square 100×100 grid. The strong coupling to the circular limiter negated the effect of the square boundary conditions. The resulting spacing is much smaller than any expected spatial phenomenon. Several simulations with higher or slightly lower resolution obtained very similar results. For every integration step, the pressure field, potential field and feedback currents are calculated. Integration from $t = 0$ to $t = 15$ takes about 30 min.

5.2. Initial and boundary conditions

In order to simplify the analysis, several assumptions were made.

- There is no end-plate biasing, and the floating potential behaves as $\varphi_w(r) = \max(0, 1 - r^2)$.
- Ion pressure is injected uniformly at every $r < 1$, with $Q_p = 4\nu_\perp^p$.

The above assumptions result in an unstable equilibrium of $\varphi(r) = \varphi_w(r)$ and $p(r) = \max(0, 1 - r^2)$. This equilibrium pressure was taken to be the initial condition of the simulation, thus avoiding an initial build-up phase. The above potential dependence dictates a rigid rotation of $\omega_{rot} = 2$, which makes our analytical model (involving rotating modes) more applicable. The initial pressure distribution has a random multimode deviation from the above equilibrium profile with a relative amplitude of 1%.

5.3. Calculating the feedback currents

For the purpose of determining the feedback currents in the simulation, knowledge of both $\varphi(x, y)$ and $p(x, y)$ was assumed. This is not a realistic assumption for real plasma experiments, but it rather follows the phase-space feedback methodology (see [13] for example). In the phase-space feedback approach one assumes a complete knowledge of all the phase-space variables of the system, and finds a feedback response based on this knowledge. A subset of the dynamical variables of the system can then be used to construct an estimator and a corresponding control law as long as the system is observable.

A temporally extrapolated electric potential is calculated by solving Poisson's equation for $\vec{\nabla}^2\varphi + \tau_{ext.} \cdot ((d/dt)\vec{\nabla}^2\varphi)_{cur.}$, with $((d/dt)\vec{\nabla}^2\varphi)_{cur.} \equiv \kappa \cdot r \cdot \hat{\theta} \cdot \vec{\nabla}p$ being the curvature-driven charge separation. This results in $\varphi_{ext.}$, an estimation

of the electric potential at time $\tau_{ext.}$ after the current time. $\vec{E}_{ext} \equiv -\vec{\nabla}\varphi_{ext.}$ is then used to determine the feedback currents' change, in analogy with equation (4):

$$\begin{pmatrix} \dot{I}_{m,x} \\ \dot{I}_{m,y} \end{pmatrix} = G \cdot \left(\begin{matrix} \langle\vec{E}_{ext.}, \vec{E}_{m,x}\rangle \\ \langle\vec{E}_{ext.}, \vec{E}_{m,y}\rangle \end{matrix} \right) + \delta \begin{pmatrix} \cos\psi & \sin\psi \\ -\sin\psi & \cos\psi \end{pmatrix} \begin{pmatrix} I_{m,x} \\ I_{m,y} \end{pmatrix}. \tag{8}$$

In this work, the feedback values used are $G = -10$, $\tau_{ext.} = 1$.

6. Simulation results

When no feedback is used, the plasma is unstable, collides with the limiter, and the total pressure ($\int p \cdot dS$) drops (top of figures 5 and 6), consistent with [9]. When feedback is turned on with $\psi = -90°$, the plasma is stable and remains at the centre of the trap regardless of δ. However, for $\delta = 0$ there are residual currents (figure 5, middle), while for $\delta = 10$ the feedback currents decay to zero (figure 5, bottom).

Figure 6 shows the total pressure as a function of time. It demonstrates the effect of the feedback in maintaining the plasma equilibrium pressure. The feedback currents are given in figure 7. The currents for the $\delta = 10$ case initially rises to suppress the initial perturbation and then drops back to near zero. The currents for the $\delta = 0$ case rise higher and remain high.

Furthermore, runs of the simulation were made for combinations of δ and ψ, with values ranging as follows: $\delta = -3, 2, \ldots, 27$ and $\psi = -160°, -120°, \ldots, 0°$. The feedback currents' decay rate is shown in figure 8. The simulated decay rate (as opposed to the analytical one defined earlier) is defined by the average decay rate of the standard deviation of the currents over half of the simulated time interval: $\tau_{decay,sim}^{-1} \equiv -(2/t_{end})\ln(I_{std}(t_{end})/I_{std}(t_{end}/2))$. A large positive decay rate means the currents decayed fast. A negative decay rate means the currents grew. The figure shows only positive values. It can be seen that both in the MHD simulation and the analytical model (figure 4), the best stabilization is obtained for the phase angle near $\psi = \pm90°$. Also, the decay rate is positive for a wide range of δ and ψ, indicating a robust feedback algorithm.

In this work, only stabilization of the $m = 1$ mode was demonstrated. This is because FLR effects are strong enough to stabilize higher m values. However, when the 'FLR' coupling coefficient (U) was lowered, the $m = 2$ mode was also unstable. With active feedback, stabilization was still achieved, but only with residual currents. Nonetheless, when the number of coils was increased to 9, the feedback currents decayed for $m = 2$ as well.

7. Summary and discussion

A scheme for using active feedback to stabilize the flute instability was investigated. The scheme consists of six coils immersed in a cold plasma, around a hot core. First, the plasma's response to current changes in a single coil was reviewed, and this response was assumed to hold for multiple (small and far-apart) coils. Then, a feedback algorithm was determined using an analytical model. This model showed that when rotation is present, and there is a demand for zero residual currents, a term proportional to the current must be added
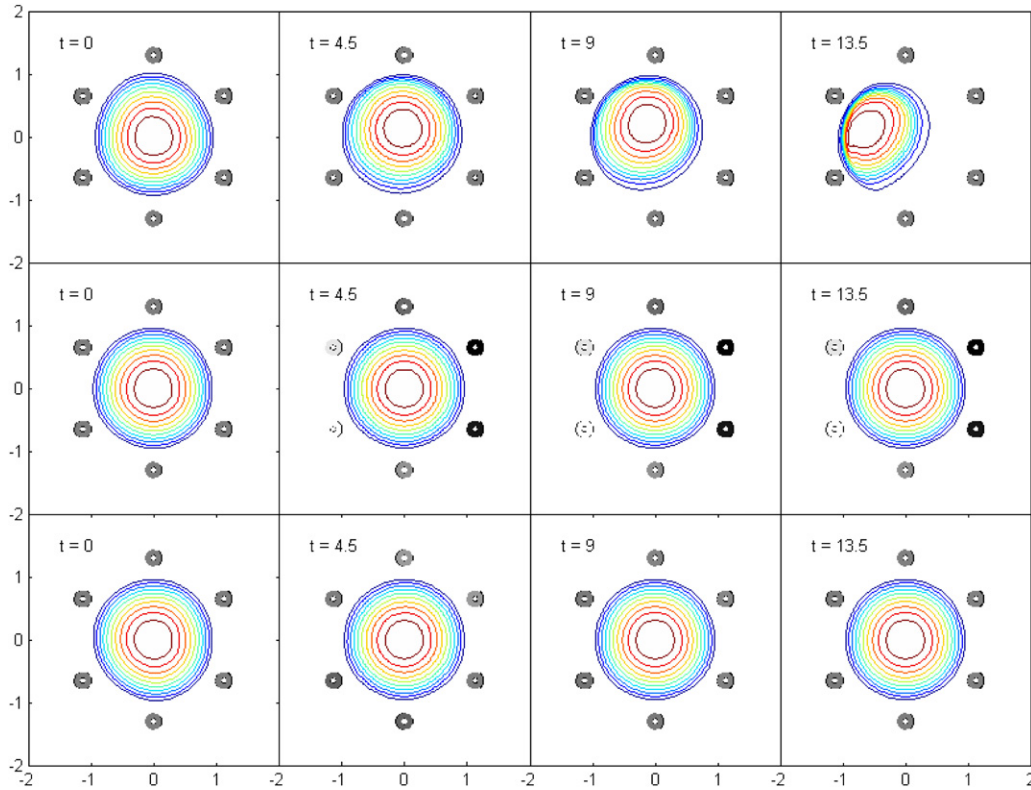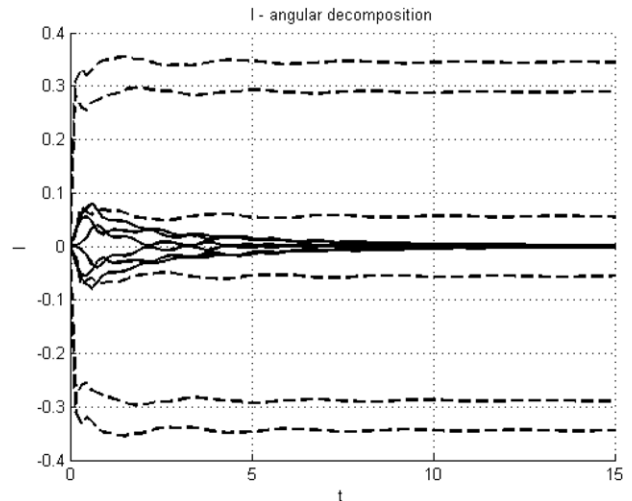
Figure 5. Pressure contour plots, with coil currents indicated by the grey level—minumum (black) is -0.4 and maximum (white) is 0.4. Top: no feedback. The plasma collides with the limiter, and there are no currents. Middle: active feedback, $\delta = 0$. The plasma is stabilized, but there are residual currents. Bottom: active feedback, $\delta = 10$, $\psi = -90°$. The plasma is stabilized with no residual currents. Snapshots taken at times 0, 4.5, 9 and 13.5 (left to right).
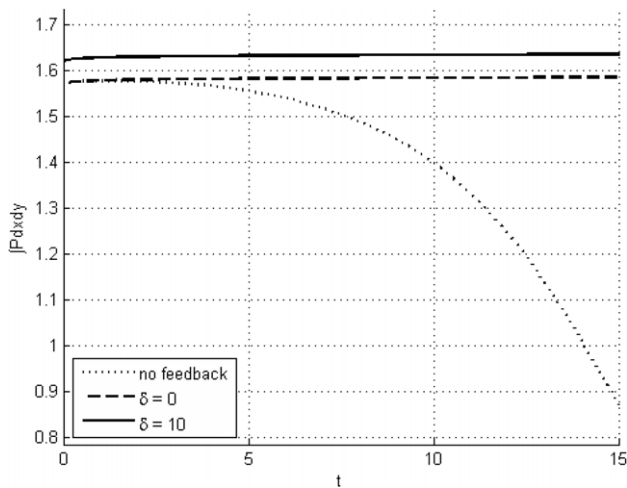
Figure 6. Total pressure ($\int p \cdot dx \, dy$) versus time. Dashed line: $\delta = 10$, $\psi = -90°$; solid line: $\delta = 0$; dotted line: no feedback. The solid line is shifted upwards to avoid overlapping with the dashed one. For the case of no feedback, there is a sudden drop when the core reaches the limiter; when feedback is used, the pressure maintains a constant value.

Figure 7. Feedback currents for each coil. Dashed lines: $\delta = 0$; solid lines: $\delta = 10$, $\psi = -90°$. Note the asymptotic decay in the latter case.

to the rate of change of the *perpendicular* current. Finally, confinement was demonstrated in a 2D MHD model when the feedback was used, with zero final currents.

It is interesting to note that the temporal limitations of the feedback coils are not due to inductance, as the plasma response is to *changes* in the feedback currents, and thus to the

loop voltage. This is crucial because the typical growth time of the flute instability is 10–$100 \, \mu$s, so any feedback system will need to be faster than this time scale.

For the small perturbations seeded in the initial pressure distribution, the normalized currents are of order unity implying feedback currents of about $B_0/\mu_0 v \approx 2.4 \, $kA. The voltage drop on the coils is of the order of
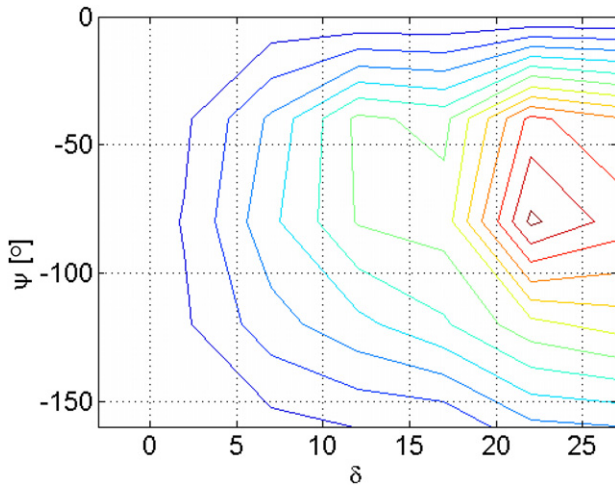
Figure 8. Contour plot of feedback currents' decay rates versus feedback parameters. Compare with the lower right quarter of figure 4. Decay rates range from 0 to 3. Contours are plotted with a 0.025 spacing.

$V_{\text{coil}} \approx \omega_{\text{typ.}} L_{\text{coil}} I \approx 6\,\text{kV}$, with $L_{\text{coil}} = \mu_0 \nu^2 L \pi R_{\text{coil}}^2$ being the coil's inductance, and assuming a normalized typical feedback current frequency of unity. Both current and voltage demands for the feedback system are achievable.

The need to immerse the coils in the plasma makes the applicability of the investigated method questionable, as it would probably result in substantial cooling and contamination of the plasma. However, the plasma around the coils is only required to be conductive enough for the mechanism of flux conservation, and can be colder than the core plasma. Such a cold plasma blanket is suggested as part of other stabilization mechanisms, such as wall stabilization [13]. Also, this work assumed full knowledge of the plasma pressure and potential, which, in practice, is limited. However, only a small number of sensors are needed to evaluate the potential [6] or density [11] components of the flute instability for the most dominant modes. A feedback scheme for a specific set of sensors can be evaluated based on the full knowledge of feedback presented in this work and common methods to construct an estimator of a dynamical system [12].

References

[1] Morozov A.I. and Solov'ev L.S. 1965 Cybernetic stabilization of plasma instabilities *Sov. Phys.—Tech. Phys.* **9** 1214–20

[2] Arsenin V.V. and Chuyanov V.A. 1977 Suppression of plasma instabilities by the feedback method *Sov. Phys.—Usp.* **20** 736–62

[3] Arsenin V.V. and Kuyanov A.Yu. 1996 Stabilization of $m = 1$ MHD modes in axisymmetric mirror devices with a $\beta \sim 1$ plasma *Plasma. Phys. Rep.* **22** 638–42

[4] Arsenin V.V. 1997 Feedback stabilization of the resistive-wall instability of a plasma in mirror systems *Plasma. Phys. Rep.* **23** 971–3

[5] Chuyanov V.A. and Murphy E.G. 1972 Feedback experiments on a high-energy plasma in the Phoenix Mirror Machine *Nucl. Fusion* **12** 177–84

[6] Zhil'tsov V.A., Kosarev P.M., Likhtenshtein V.K., Panov D.A., Chuyanov V.Y. and Shcherbakov A.G. 1977 Limitations on the plasma density in the Ogra-3 device *Sov. J. Plasma Phys.* **3** 20–5 (Engl. transl.)

[7] Chu M.S., Chance M.S., Glasser A.H. and Okabayashi M. 2003 Normal mode approach to modelling of feedback stabilization of the resistive wall mode *Nucl. Fusion* **43** 441

[8] Liu Y., Chu M.S., Garofalo A.M., La Haye R.J., Okabayashi M., Pinches S.D. and Reimerdes H. 2006 Modeling of resistive wall mode and its control in experiments and ITER *Phys. Plasmas* **13** 056120

[9] Beklemishev A.D., Bagryansky P.A., Chaschin M.S. and Soldatkina E.I. 2010 Vortex confinement of plasmas in symmetric mirror traps *Fusion Sci. Technol.* **57** 351–60

[10] Cohen B.I., Freis R.P. and Newcomb W.A. 1986 Interchange, rotational, and ballooning stability if long-thin axisymmetric systems with finite-orbit effects *Phys. Fluids* **29** 1558–77

[11] Anikeev A.V., Bagryansky P.A., Ivanov A.A., Kuzmin S.V. and Salikova T.V. 1992 Experimental observation on non-MHD effects in the curvature driven instability *Plasma Phys. Control. Fusion* **34** 1185–99

[12] Franklin G.F., Powell J.D. and Emami-Naeini A. 1995 *Feedback Control of Dynamic Systems* 3rd edn (Reading, MA: Addison-Wesley)

[13] Segal D., Wickham M. and Rynn N. 1982 Flute stabilization by cold line-tied blanket *Phys. Fluids* **25** 1485–7